First Firing of a 100-kW Nested-channel Hall Thruster

IEPC-2013-394

Presented at the 33rd International Electric Propulsion Conference,
The George Washington University • Washington, D.C. • USA
October 6 – 10, 2013

Roland E. Florenz[*], Scott J. Hall[†], and Alec D. Gallimore[‡]
University of Michigan, Ann Arbor, MI, 48109, U.S.A.

Hani Kamhawi[§] and Christopher M. Griffiths[**]
NASA Glenn Research Center, Cleveland, OH, 44135, U.S.A.

Daniel L. Brown[††]
Air Force Research Laboratory, Edwards AFB, CA, 93523, U.S.A.

and

Richard R. Hofer[‡‡] and James E. Polk[§§]
NASA Jet Propulsion Laboratory, Pasadena, CA, 91109, U.S.A.

Abstract: Currently, there is interest in scaling electric propulsion devices to higher power from 30 kW to 300 kW. An effective method of meeting this call is investment in extending the power range of mature technology. Both the Air Force and NASA have determined nested-channel Hall-effect thrusters (NHTs) are a promising path forward[1]. The X3 NHT, a 100-kW class laboratory model thruster, has been designed and fabricated leveraging past high-power HETs as well as proof-of-concept work by Liang in order to provide a benchmark NHT device Developed jointly by the University of Michigan Plasmadynamics and Electric Propulsion Laboratory (PEPL), Air Force Research Laboratory, NASA Glenn Research Center and NASA Jet Propulsion Laboratory, the X3 NHT is a three-channel NHT with a nominal power throttling range from 1 kW to >200 kW. Based on conventional thruster scaling, to the X3 may achieve 15 N of thrust and 4,600 sec of Isp with xenon and krypton propellant, respectively. In this paper we preview the initial operation of the 100-kW class NHT.

Nomenclature

g_0 = gravitational constant at Earth's surface

[*] Ph.D. Candidate, Department of Aerospace Engineering, rflorenz@umich.edu
[†] Ph.D. Pre-Candidate, Department of Aerospace Engineering, sjhall@umich.edu
[‡] Arthur F. Thurnau Professor, Department of Aerospace Engineering, and Director of the Plasmadynamics and Electric Propulsion Laboratory, alec.gallimore@umich.edu
[§] Research Engineer, Propulsion and Propellants Branch, hani.kamhawi-1@nasa.gov
[**] Senior Mechanical Designer, ASRC Aerospace Corporation, Christopher.M.Griffiths@nasa.gov
[††] Program Manager, High-Power Electric Propulsion Group, daniel.brown.50@us.af.mil
[‡‡] Senior Engineer, Electric Propulsion Group, Richard.r.hofer@jpl.nasa.gov
[§§] Principal Engineer, Propulsion and Materials Engineering Section, james.e.polk@jpl.nasa.gov

$I_{D,AC(t)}$ = AC component of channel discharge current
$I_{D,mean}$ = mean channel discharge current
$I_{D,pk\text{-}pk}$ = peak-to-peak channel discharge current oscillation

I_{sp} = specific impulse
P = thruster electrical power input
T = thrust
T/P = thrust to power ratio
η = Thruster efficiency in converting electrical power to directed kinetic power

I. Introduction

NESTING the channels of Hall thrusters has proven to be a viable method to increase discharge power and propellant throughput in a compact form factor. Nested-channel Hall thrusters (NHTs) not only process increased power, but have decreased footprint compared to comparable single-channel Hall thrusters or clusters thereof. In addition, flexibility in channel operation and discharge current density (and power density) allows both "high-thrust" and high-specific impulse (I_{sp}) configurations at a constant power level.

Proof-of-concept work by Liang[2] included building and testing the two-channel, 10-kW-class NHT called the X2. Building upon his work, the Plasmadynamics and Electric Propulsion Laboratory (PEPL) at the University of Michigan, with the support of the United States Air Force Office of Scientific Research (AFOSR), Air Force Research Laboratory (AFRL) and NASA, has designed, built, and fired a 100-kW-class three-channel NHT known as the X3. This thruster has three discharge channels and seven distinct operating regimes comprised of combinations of channel operation (i.e., 1, 2 or 3 channels on) and discharge voltage and current. It is expected to achieve 4,600 s of I_{sp} at high discharge voltage and 15 N of thrust at moderate I_{sp} on krypton and xenon propellant, respectively.

Presented here are the results of the initial firing of the X3 NHT on krypton, performed at PEPL in the Large Vacuum Test Facility (LVTF). Each channel was fired individually at a discharge voltage of 300 V, followed by the various combinations of channels at the same discharge voltage. The objectives of this firing were to "burn-in" the thruster channels and to optimize the electromagnet coil currents at each thruster setting for stability.

The paper is organized as follows. In Section II, we motivate the design, fabrication, and ground testing of high-power EP devices. In Section III, a brief description of the heritage of the X3 NHT is laid out for the reader. In Section IV, the experimental setup including the thruster and support equipment is described. In Section V, observations of the operation of the X3 are given. Finally, we conclude in Section VI with some over-arching observations and provisions for the next steps of testing.

II. Motivation

In recent years, there has been a steadily building interest in developing high-power EP devices.[3-5] Such systems (~100 kW to ~1 MW) have been flagged as a high-priority technology per the 2012 *NASA Space Technology Roadmaps and Priorities.*[6] Recently, a NASA Solar Electric Propulsion (SEP) Demonstration Mission Concept Studies broad agency announcement (NNC11ZMA017K) awarded contracts for teams to conduct concept and mission studies of advancing key in-space propulsion concepts for a 300-kW SEP vehicle.[7] The European Union, meanwhile, has been funding the HiPER (High-power Electric propulsion: Roadmap for the future) project to lay the groundwork for Europe's future space transportation and exploration needs.[8]

Future space missions with large ΔVs favor the use of EP, whose large I_{sp} relative to chemical propulsion reduces required propellant mass for a given mission, thereby boosting payload mass fraction and/or reducing launch costs. In an EP system, the I_{sp} and thrust T are related to thruster electrical power input, P, by

$$P = (g_0 \, I_{sp} \, T)/(2 \, \eta) \qquad (1)$$

where g_0 is the gravitational constant at Earth's surface and η is the thruster efficiency in converting electrical power to directed kinetic power. Time-critical missions such as human spaceflight[9] require short flight times. Use of EP either for transporting astronauts or the infrastructure they need to complete their mission (i.e., SEP cargo vessel) drive the requirement for high-power (>100 kW) EP.

Example missions enabled by high-power EP include:

- Cargo tugs cycling between Low Earth Orbit (LEO) and High Earth Orbit for on-station deployment of satellites[10] (e.g., in Geosynchronous Earth Orbit, GEO) or to support lunar and Martian exploration missions;[11]
- Heliocentric orbit transfer vehicles to Near Earth Objects (NEO)[12] and Mars;[13-16]
- Solar system exploration missions, such as the Jupiter Icy Moons Orbiter[17] envisioned under Project Prometheus;
- International Space Station orbit re-boost to provide drag makeup in LEO;[18] and
- Orbital power beaming systems[19] that require drag makeup in LEO or transfer to higher orbits.

These missions in the hundreds of kW range are possible due to advancements in photovoltaic arrays[20] (e.g., Boeing's FAST arrays[21]) and solar concentrators. Missions requiring even higher power levels would likely need to make use of high specific power nuclear reactors.[22]

These trends in space power for Earth-centric missions are also helping to drive USAF interests in high-power EP. The USAF has invested in high-power plasma propulsion research and development via the University of Michigan/Air Force Center of Excellence in Electric Propulsion (MACEEP),[23] through which the dual-channel X2 proof-of-concept Nested Hall Thruster[24] (NHT), the three-channel X3 NHT,[25] and the Electrodeless Lorentz Force (ELF)[26] thruster are being developed.[***]

III. Brief Overview of the Heritage of the X3 NHT

Hall Thrusters have displayed an increase in size and power since first being launched by the Russians in the 1970's. Modern single-channel Hall thrusters have demonstrated power levels ranging from 200 W (e.g., Busek's BHT-200) to just shy of 100 kW (the NASA-457M) while achieving specific impulses ranging from 1000 to 5000 s, efficiencies greater than 60%, and thrust-to-power ratios (T/P) up to the mid-90 mN/kW range.[27-32] The X2 NHT was developed as a proof-of-concept device for nesting channels as a means to increase power and throttleability while limiting the increase of thruster mass. The X3 NHT design heritage traces to the X2 NHT, H6 Hall thruster, and leverages lessons learned in developing the NASA high-power single-channel Hall thrusters (i.e. NASA-457M, -400M and -300M).[33]

Figure 1 A selection of NASA Hall Thrusters

[***] ELF thruster development was initially part of the Center.

IV. Experimental Setup

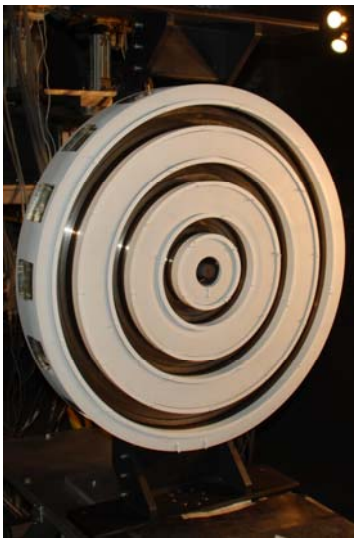

Figure 2 X3 NHT.

A. X3 NHT

The X3 NHT is a three-channel NHT pictured in Figure 2. Capable of operating over a range of discharge voltages of 200 to 800 V, the test matrix presented in this paper covers only the initial 300-V operation of the thruster. All seven configurations of the thruster were tested, with the channels operating at a constant discharge current density. This current density is derived from all three channels operating simultaneously with a total discharge current of 100 A. The X3 utilizes a centrally-mounted cathode. For the entirety of operation points presented in this document, a Lanthanum Hexaboride (LaB6) cathode provided by the NASA Jet Propulsion Laboratory (JPL) rated to over 250 A was used.

The test matrix for the thruster is provided in Table 1**Error! Reference source not found.** below.

Table 1. X3 NHT First Firing Test Matrix. I=Inner,M=Middle, O=Outer, Kr=Krypton

Channel(s)	Power [kW]	Discharge Voltage [V]	Discharge Current [A]	Propellant
I	**3.9**	**300**	**13.1**	**Kr**
M	**9.6**	**300**	**31.9**	**Kr**
O	**16.5**	**300**	**55.1**	**Kr**
I+M	**13.5**	**300**	**45.0**	**Kr**
M+O	**26.1**	**300**	**87.0**	**Kr**
I+O	**20.5**	**300**	**68.2**	**Kr**
I+M+O	**30.0**	**300**	**100.1**	**Kr**

B. Facility and Telemetry Monitoring

The X3 NHT was installed and tested in the LVTF (Figure 3). The LVTF is a 200 m^3 stainless-steel-clad vacuum chamber 9 m long and 6 m in diameter. Rough vacuum is achieved using two 2000 CFM blowers backed by four 400 CFM mechanical roughing pumps with a final base pressure in the low 10^{-7} Torr achieved through the use of seven CVI-TM1200 internal cryopumps with LN2 shrouds that provide a nominal pumping speed of about 500,000 l/s on air and 250,000 l/s on krypton. During operation, chamber pressure is measured by an external ion gauge at the top of the chamber axially co-located with the thruster exit plane with an uncertainty of +/- $1x10^{-7}$ Torr. The pressure varied in the chamber during testing due to changing anode and cathode flow rates with a fixed pumping speed.

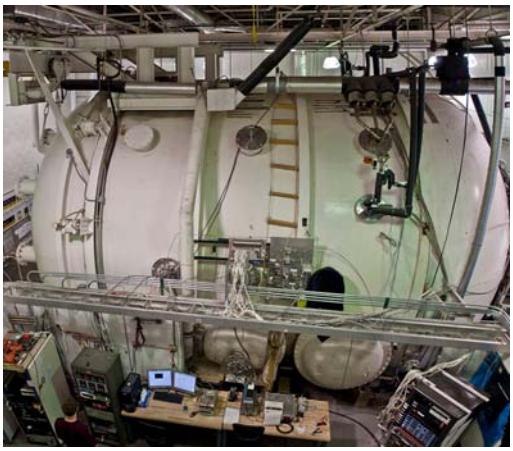

Figure 3 Large Vacuum Test Facility

Power was supplied to the inner, middle and outer channels of the thruster by a Magnapower 60-kW DC power supply, an Amrel 100-kW DC power supply, and a Magnapower 150-kW DC power supply, respectively. This discharge power was supplied across two 160-μF 1000-V Cornell Dubilier polypropelene film capacitors per channel. The mean discharge current for the inner and middle channel was measured with a CDR-100 FW-Bell magneto-resistive current sensor each, while the outer channel discharge current was measured by a CDR-150 magneto-resistive current sensor. Discharge voltages were measured via sense lines attached directly to the anodes and cathode and fed into 201:1 voltage dividers comprised of low-inductance metal-oxide film resistors. Magnet coil currents were read across 30-A, 100-mV current shunts (Deltec WB-30-100). Magnet voltages were read directly off of the output side of the power/telemetry breakout box pictured in Figure 4.

Keeper current was measured across a Deltec WB-10-100 10 A, 100 mV current shunt and its voltage was put through a 101:1 voltage divider. Heater current was measured across a Deltec WB-30-100 30 A, 100 mV current shunt and voltage was measured directly at the output side of the power/telemetry breakout box. All telemetry signals were routed to an Agilent 34970A Data Acquisition/Switching unit. Voltage measurements were calibrated using a BK precision 5491A multimeter. Current measurements were calibrated using a precision 10-mOhm resistor accurate to 0.1% and a BK precision 5491A multimeter. Plume photographs were taken with a Nikon D3200 and a Nikon D80 digital camera.

Alicat Scientific MC Series mass flow controllers are used to deliver the krypton propellant to the X3 through electro-polished stainless steel lines. A Bios Definer 220L DryCal system plumbed in parallel to the anode and cathode feed lines, with a measurement accuracy of 1% of the reading between 5 and 500 sccm, is used for mass flow calibration. Mass flow calibration is done for each controller at multiple points and a linear fit is performed. This linear fit is used to determine the flow at any arbitrary set point. The AC component of each channel's discharge current, ID,AC(t), was measured with a Tektronix TCP 303 (DC to 15-MHz bandwidth) split-core Hall current sensor through a Tektronix TCPA 300 current probe amplifier. The signal was measured on the discharge current line external to the chamber on the anode side for each respective channel.

Figure 4 X3 NHT power and telemetry breakout box.

V. Observations of Thruster Operation

During the initial testing of the X3, diagnostic evaluation of the thruster was limited to two means. The first is that of photographic interrogation with the use of the DSLR cameras as described in the section above to assess the overall quality of the plume; e.g. identify hot spots. The second avenue of approach is that of high-speed measurement of the discharge current to provide a more quantitative evaluation of the stability of the discharge. The base telemetry for each condition is presented in

Table 2 below.

Table 2. Telemetry of X3 at all operating conditions. *Note: corrected for Krypton.

Channel(s)	Total Power [kW]	Discharge Current [A]	Discharge Voltage [V]	Total Mass Flow Rate [mg/s]	*Pressure [Torr]
I	3.9	13.0	300.5	9.2	1.0×10^{-5}
M	9.6	32.0	299.8	21.2	2.3×10^{-5}
O	16.5	55.1	299.6	36.1	3.6×10^{-5}
I+M	13.4	44.6	300.2	24.4	2.1×10^{-5}
I+O	21.1	70.3	300.6	40.7	3.5×10^{-5}
M+O	26.1	87.1	299.4	49.4	5.0×10^{-5}
I+M+O	30.0	100.1	299.7	53.9	6.1×10^{-5}

An interesting observation that can be made from this table is that less mass flow is required to maintain a given channel mean discharge current as each additional channel is turned on. Without performance measurements, it is

not possible to draw any conclusions about whether or not this is a positive or negative effect. However, it is indicative of channel interactions as characterized by Liang[34].

A. Photographic Evaluation

In order to provide a qualitative understanding of the structure of the plasma and the stability of the thruster, two DSLR cameras were employed. One camera was positioned looking down the thrust axis of the X3 at an acute angle (camera 1) and the other providing a side view of the thruster (camera 2).

The purpose of camera 1 was to provide an understanding of any hot spots that might develop in the thruster as well as detect any azimuthal nonuniformities in the plume. Hot spots can be defined as any locations on the channel walls or anode itself that are substantially brighter than the rest of that given channel, and possibly might even glow red to indicate some form of preferential heating. Azimuthal non-uniformities could take the form of peaks and valleys of brightness in the discharge, either periodic or aperiodic. Referring to Figure 5, we can see that neither hot-spots nor azimuthal non-uniformities are present across all seven operating modes.

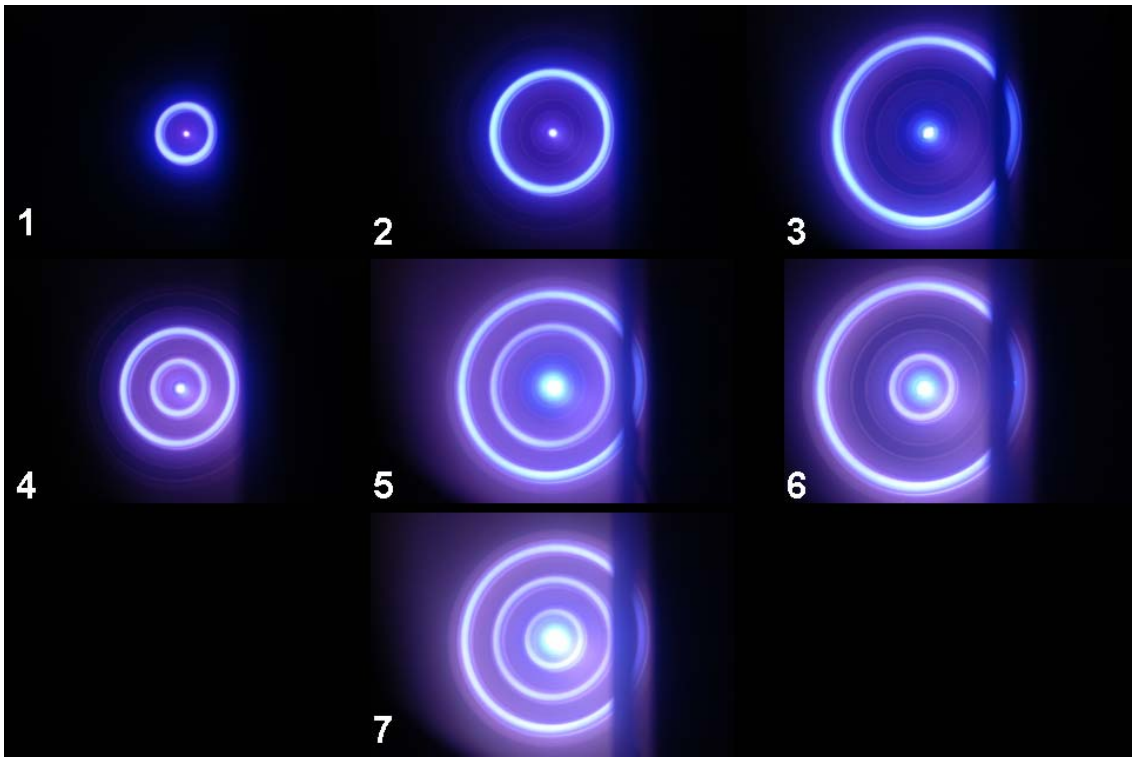

Figure 5 All operating modes of the X3 (front view). Operating points from top-left to bottom-right: (1) Inner, (2) Middle, (3) Outer, (4) Inner+Middle, (5) Middle+Outer, (6) Inner+Outer, (7) Inner+Middle+Outer. All photographs were taken with the same camera settings. The black bar seen in (5), (6), and (7) is a physical part of the chamber (shutter-like beam dump at the downstream endcap).

Camera 2 was employed to give another perspective on the structure of the plume and to allow detection of any anomalous coupling of the plume to the facility. From this side-view, it would be possible to detect azimuthal non-uniformities in terms of discharge brightness that could signal the discharge favoring the top (thruster 12 o'clock) or bottom (thruster 6 o'clock) of the frame. An example of anomalous coupling of the plume to the facility would be the plume coupling to the metal grating directly downstream of the thruster, which would be evidenced by a distinct

downward arc of the plume in any of the images from camera 2. None of these abnormalities were observed during thruster operation as one can see in Figure 6. The plume is qualitatively symmetric across all seven conditions.

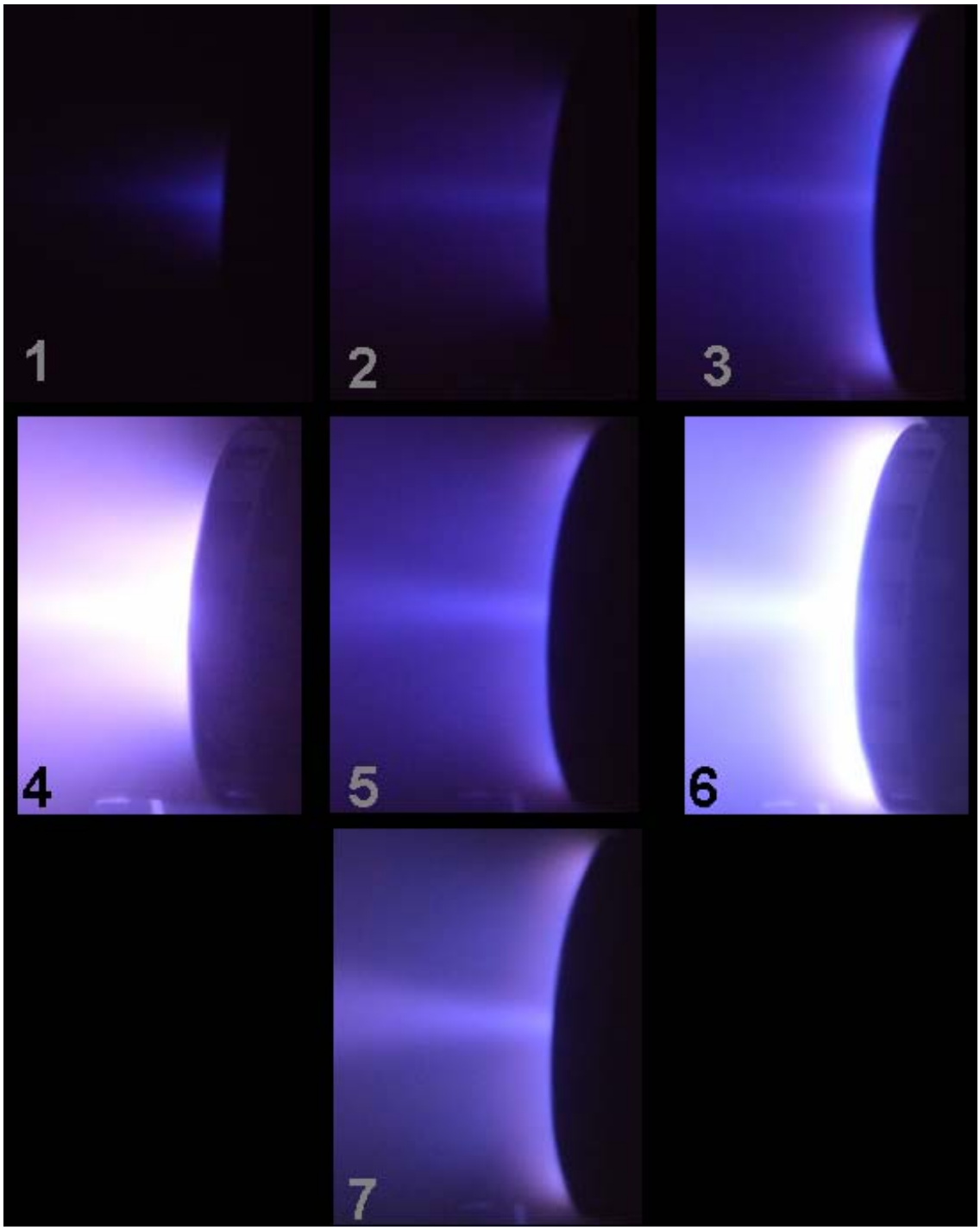

Figure 6 All operating modes of the X3 (side view). Operating points from top-left to bottom-right: (1) Inner, (2) Middle, (3) Outer, (4) Inner+Middle, (5) Middle+Outer, (6) Inner+Outer, (7) Inner+Middle+Outer. All photographs were taken with the same camera settings with the exception of those for operating points (4) and (6), which are over-exposed.. In actuality, the plume brightness for operating points (4) and (6) is comparable to that of (5).

B. High-speed current probe evaluation

Through the independent monitoring of each discharge channel on the anode side of the circuit, we are able to observe high-frequency oscillations (kHz and above) that the naked eye and the two DSLR cameras cannot. This provides another tool for determining the stability of the thruster as well as offering a means for understanding interaction between channels.

Both qualitative and quantitative metrics were employed to determine stability during testing. The first is to say the less structure the oscillations had the better the thruster was operating. During these evaluations, the oscilloscope was sampling in the range of 1-2 giga-samples per second. Structure, in the case of discharge current, is a trace that approximates a sinusoid. When observing the post-processed power spectral densities (PSDs), this takes the form of a trace that has no prominent peak. From empirical observation, this was determined to be more stable because the more sinusoidal the oscillations became, it was found that there was a higher probability of the oscillations of the thruster growing to a damaging amplitude. It should be noted that there are modes where the thruster will not go unstable even if the AC-coupled current trace takes a distinctly sinusoidal form. Quantitatively speaking, as long as the mean peak-peak oscillations are kept to under 15% of the mean discharge current, the thruster can be considered in a comfortable operating regime. The exception to this rule is the inner channel, which seems to sit at an oscillation amplitude of higher magnitude. The wording here is purposely chosen as ambiguous as this thruster is still in its early stages of operation and may yet change. Further, there were extended periods of operation (>30 minutes) where the mean peak-peak oscillation was observed to be less than what shown here. No telemetry was taken at those points and thus they are not reported here.

The plots in Figure 7 below are the power spectral densities of the raw data from the oscilloscope with minimal smoothing. The post-processing was done in Matlab via the built-in PSD functionality.

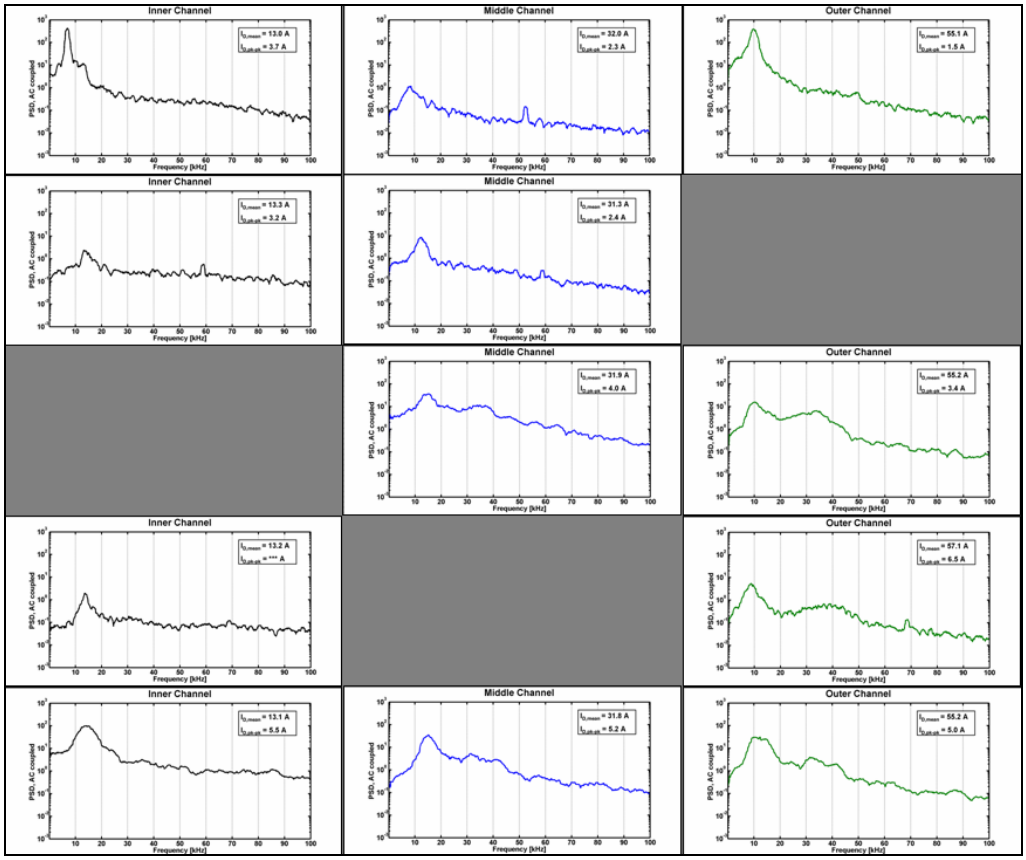

Figure 7 AC-coupled power spectral densities (PSDs) of the discharge currents. The first row of plots is each individual channel operating by itself. The conditions for the following four rows are top to bottom are: (4), (5), (6), (7). Columns left-right are: inner, middle, outer channel respectively.

A number of observations can be made from looking at these plots. First, we note that all three channels have a fundamental oscillation frequency in the 5-10 kHz range, increasing from inner to outer channel. Based on the peak-peak oscillation amplitude, we can also note that all three channels are remarkably "quiet", with the inner channel being the "noisiest." Here "quiet" is defined as a having a peak-peak amplitude that is a relatively low percentage of mean discharge current.

Perhaps of greater interest, however, are the preliminary observations that can be made about channel interaction. As more channels are added, we can see that the PSD magnitude broadens across the frequency range with the damping out of any prominent peaks, with the greater broadening occurring when adjacent channels are turned on. What peak frequency does exist is moved to the right into a value that is higher than either of the independent channel oscillation frequencies. We can note that, for example, with all three channels running together the oscillations have shifted to approximately 15 kHz and even the magnitude of the oscillations seem to have synced up with peak-peak values at essentially 5 A. It seems that in this case, the amplitude of the outer channel's oscillations drive that of the inner two, while all three channels convolve together to form a new fundamental frequency not explicitly organic to any of them.

VI. Conclusions and Next Steps

There are many significant conclusions to be made from just these few initial operating points of the X3. First is that three concentrically nested channels can simultaneously be operated off of a single centrally mounted cathode without compromising thruster stability. All seven thruster conditions have initially been shown to behave as expected, without azimuthal non-uniformities and without strong high frequency oscillations that negatively impact the thrusters ability to stay lit. Through the use of high-speed current probes, we are able to preliminarily say that there is a distinct coupling that occurs between each channel as it is operated in concert with the others. This occurs both in the form of altering oscillation frequencies and amplitudes. This is further supported from the simple telemetry that says that individual anode mass flow rates can be reduced as each additional channel is engaged in order to maintain each channel's single-channel discharge current level, a "cross-utilization" of propellant of sorts. This preliminary observation is consistent with Liang's 2-channel studies.

What cannot yet determine how well the thruster is operating in terms of performance. In addition, the observed cross-utilization of propellant between channels cannot be deemed an indicator of increased performance. Further, thruster stability across its full discharge voltage and current range has not yet been assessed. Lastly, a qualifier must be attached to the conclusions and observations contained in this paper: the shape of the applied magnetic field was left constant across all operating conditions. Variation of this shape might very well alter the operation, with towards and away from stability being equally probable.

Thus, the immediate next steps for thruster testing are as follows. First, all of the operating modes will be tested at increasing discharge voltages up to 550 VDC, with the option of increasing as high as 800 VDC. These higher voltages will still be operated on krypton propellant. That will conclude the shakedown phase of thruster testing. After that is completed, the X3 will be installed on PEPL's thrust-stand located in the LVTF to determine its performance in terms of thrust produced at each given operating condition, optimizing magnetic field configuration at each condition respectively. During this phase of evaluation, xenon will be the primary propellant used.

Acknowledgments

The authors would like to thank the following individuals and organizations for their support and contributions: Dr. Mitat Birkan of the Air Force Office of Scientific Research, Dr. James Haas of the Air Force Research Laboratory (AFRL), Dr. Peter Peterson of the Aerojet-Rocketdyne Corporation (at the time of his work, of ElectroDynamic Applications, Inc), Mr. Kevin Blake of NASA GRC, and Mr. Joseph Blakely of AFRL. Without their help and support this work would not have been possible. Roland Florenz is funded by the Michigan AFRL Center for Excellence in Electric Propulsion and the Michigan Space Grant Consortium. Scott Hall is funded by a fellowship from the National Science Foundation.

References

[1] 1Brown, D., Beal, B. and Haas, J., "Air Force Research Laboratory high power electric propulsion technology development," *IEEE Aerospace Conference*, 2010, pp. 1-9.

[2] Liang, R. and Gallimore, A.D., "Far-Field Plume Measurements of a Nested-Channel Hall-Effect Thruster." *49th AIAA Aerospace Sciences Meeting including the New Horizons Forum and Aerospace Exposition, Orlando, Florida*, AIAA-2011-1016. Jan. 4-7, 2011

[3] Jankovsky, R., Tverdokhlebov, S., and Manzella, D., *"*"High-power Hall thrusters.*"*" AIAA-1999-2949, 35th AIAA/ASME/SAE/ASEE Joint Propulsion Conference and Exhibit, Loss Angeles, CA, June 20, 1999.

[4] Jacobson, David T., and Jankovsky, Robert S., *"*"Performance evaluation of a 50 kW Hall thruster.*"*" AIAA-1999-457, 37th Aerospace Sciences Meeting and Exhibit, Reno, NV, January 11, 1999.

[5] Jacobson, D., Manzella, D., Hofer, R., and Peterson, P., *"*"NASA's 2004 Hall Thruster Program.*"*" AIAA-2004-3600, 40th AIAA/ASME/SAE/ASEE Joint Propulsion Conference and Exhibit, Fort Lauderdale, Florida, July 11, 2004.

[6] 2012 *NASA Space Technology Roadmaps and Priorities*

[7] National Aeronautics and Space Administration, Glenn Research Center *"*"Solar Electric Propulsion System Demonstration Mission Concept Studies,*"*" Broad Agency Announcement, BAA NNC11ZMA017K, June 21, 2011.

[8] C. Casaregola, G. Cesaretti, and M. Andrenucci, "HiPER: a Roadmap for Future Space Exploration with innovative Electric Propulsion Technologies," IEPC-2009-066.

[9] Strange, N., Landau, D., Polk, J., Brophy, J., and Mueller, J., *"*"Solar Electric Propulsion for a Flexible Path of Human Exploration.*"*" 61st International Astronautical Congress, 2010.

[10] Gulczinski, F. S., and Schilling, J. H. "Comparison of Orbit Transfer Vehicle Concepts Utilizing Mid-Term Power and Propulsion Options," International Electric Propulsion Conference, IEPC-03-022. Toulouse, France, 2003.

[11] Andrews, D. G., and Wetzel, E. D. "Solar Electric Space Tug to Support Moon and Mars Exploration Missions " Space 2005 Conference & Exhibit, AIAA-05-6739. AIAA, Long Beach, California, 2005.

[12] Brophy, J., Gershman, R., Strange, N., Landau, D., Merrill, R., and Kerslake, T., *"*"300-kW Solar Electric Propulsion System Configuration for Human Exploration of Near-Earth Asteroids.*"*" AIAA-2011-5514, 47th AIAA/ASME/SAE/ASEE Joint Propulsion Conference and Exhibit, San Diego, California, July 31, 2011.

[13] Dankanich, J. W., Vondra, B., and Ilin, A. V. "Fast Transits to Mars Using Electric Propulsion," Joint Propulsion Conference, AIAA-10-6771. Nashville, Tennessee 2010.

[14] Strange, N., Merril, R., Landau, D., Drake, B., Brophy, J., and Hofer, R., *"*"Human Missions to Phobos and Deimos Using Combined Chemical and Solar Electric Propulsion.*"*" AIAA Paper 2009-5663, July, 2011.

[15] Donahue, B., *"*"Solar Electric and Nuclear Thermal Propulsion Architectures for Human Mars Missions Beginning in 2033.*"*" AIAA-2010-6819, 46th AIAA/ASME/SAE/ASEE Joint Propulsion Conference and Exhibit, Nashville, TN, July 25, 2010.

[16] Frisbee, R., *"*"Evaluation of High-power Solar Electric Propulsion Using Advanced Ion, Hall, MPD, and PIT Thrusters for Lunar and Mars Cargo Missions.*"*" AIAA-2006-4465, 42nd AIAA/ASME/SAE/ASEE Joint Propulsion Conference and Exhibit, Sacramento, California, July 9, 2006.

[17] Randolph, T., Dougherty, R., Oleson, S., Fiehler, D., and Dipprey, N., *"*"The Prometheus 1 Spacecraft Preliminary Electric Propulsion System Design.*"*" AIAA-2005-3889, 41st AIAA/ASME/SAE/ASEE Joint Propulsion Conference and Exhibit, Tucson, Arizona, July 10, 2005.

[18] Oleson, S.R. and Benson, S.W., "Electric Propulsion for International Space Station Reboost: A Fresh Look," AIAA-2001-3644, 37th AIAA/ASME/SAE/ASEE Joint Propulsion Conference and Exhibit, Salt Lake City, Utah, July 8-11, 2001.

[19] Komerath, N.M; Boechler, N. (October 2006). The Space Power Grid. Valencia, Spain: 57th International Astronautical Federation Congress. IAC-C3.4.06.

[20] Mikellides, I., and Jongeward, G., "Assessment of High-Voltage Solar Array Concepts for a Direct Drive Hall Effect Thruster System." AIAA-2003-4725, 39th AIAA/ASME/SAE/ASEE Joint Propulsion Conference and Exhibit, Huntsville, Alabama, July 20, 2003.

[21] Defense Advanced Research Programs Agency, Tactical Technology Office, *"*"Fast Access Spacecraft Testbed (FAST),*"*" Broad Area Announcement, BAA 07-65, 2007.

[22] Randolph, T., Dougherty, R., Oleson, S., Fiehler, D., and Dipprey, N., "The Prometheus 1 Spacecraft Preliminary Electric Propulsion System Design." *AIAA-2005-3889*, 41st AIAA/ASME/SAE/ASEE Joint Propulsion Conference and Exhibit, Tucson, Arizona, July 10, 2005.

[23] *"*"Michigan/Air Force Center of Excellence in Electric Propulsion (MACEEP)*"*", http://www.umich.edu/~peplweb/maceep.html, 26 June 2011.

[24] Liang, R. and Gallimore, A.D., *"*"Far-Field Plume Measurements of a Nested-Channel Hall-Effect Thruster." 49th AIAA Aerospace Sciences Meeting including the New Horizons Forum and Aerospace Exposition, Orlando, Florida, AIAA-2011-1016. Jan. 4-7, 2011

[25] Roland Florenz, Alec D. Gallimore, Peter Y. Peterson, "Developmental Status of a 100-kW Class Laboratory Nested channel Hall Thruster," IEPC-2011-246, 32nd International Electric Propulsion Conference, Wiesbaden , Germany, September 11 – 15, 2011.

[26] Slough, J., Kirtley, D., and Weber, T., "Pulsed Plasmoid Propulsion: The ELF Thruster," IEPC-2009-265, 31st International Electric Propulsion Conference, Ann Arbor, MI, September 20-24, 2009.

[27] Jacobson, D., and Manzella, D., "50 kW Class Krypton Hall Thruster Performance," Joint Propulsion Conference, AIAA-03-4550, AIAA, Huntsville, Alabama, 2003.

[28] Peterson, P., Jacobson, D., Manzella, D., and John, J. W. "The Performance and Wear Characterization of a High-Power, High-Isp NASA Hall Thruster," Joint Propulsion Conference, AIAA-05-4243, AIAA, Tucson, Arizona, 2005.

[29] Manzella, D., Oh, D., and Aadland, R. "Hall Thruster Technology for NASA Science Missions," Joint Propulsion Conference, AIAA-05-3675, AIAA, Tucson, Arizona, 2005.

[30] Manzella, D., and Jacobson, D. “Investigation of Low-Voltage/High-Thrust Hall Thruster Operation,” Joint Propulsion Conference, AIAA-03-5004, AIAA, Huntsville, Alabama, 2003.

[31] Manzella, D. “Low Cost Electric Propulsion for Deep Space Robotic Missions,” NASA Science Technology Conference, Adelphi, Maryland, 2007.

[32] Manzella, D., Jankovsky, R., and Hofer, R. “Laboratory Model 50 kW Hall Thruster,” Joint Propulsion Conference, AIAA-02-3676, a ed., AIAA, Indianapolis, Indiana, 2002.

[33] Kamhawi, H., Haag, T. W., Jacobson, D. T., & Manzella, D. H. “Performance Evaluation of the NASA-300M 20 kW Hall Effect Thruster”. National interest, 220(8), 9, 2011.

[34] Liang, R., "**The Combination of Two Concentric Discharge Channels into a Nested Hall-Effect Thruster**," Ph.D. Dissertation, University of Michigan, 2013.